

Study of Structural Investigation and Opto Electronic Properties of Titania Nanoparticles with the Impact of Amino-Acids by Microwave Irradiation Method at High Temperature

Praveena Paneerselvam¹, Vadamarathinam^{2*}, Hemavathi A³

¹ PG and Research Department of Physics, Muthurangam Government Arts College, Tamil Nadu, India

^{2*} PG and Research Department of Physics, Muthurangam Government Arts College, Tamil Nadu, India

³ Department of Physics, D.L.R. College of Arts And Science, Tamil Nadu, India

¹PraveenaPhysics89@gmail.com

^{2*}yadamalarvnb@yahoo.co.in

³Hemav_12@yahoo.com

ABSTRACT

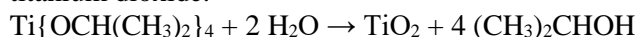
In this study, Titania nanoparticles (TiO₂) and Titanium dioxide influenced with Glycine and Alanine (T:G:A) nanoparticles have been synthesized by Microwave-Irradiated method at high temperature. Its Structural investigation and opto electronic properties are carried at 400°C. The synthesized Nanoparticles are characterized by X-Ray Diffraction, FTIR, UV-VIS, FE-SEM. The Structural Investigation of the synthesized Titania (TiO₂ and T:G:A) Nanoparticles are obtained from X-Ray diffraction Analysis. Crystal Structure having (hkl) orientation with the crystallite size (D), Dislocation density (δ), Strain, Specific Surface Area (SSA) their Inter-relationships of Morphology Index (M.I.) have been studied. The various intensity peaks of functional group obtained at the different modes of vibration is revealed by Fourier Transformation Infra-red (FTIR) Analysis. The Optical Absorption and energy band gap of the TiO₂ and T:G:A nanoparticles was calculated using UV-visible spectroscopy Studies. The morphological survey was found to be Spherical in shape and agglomerated

Key Words: TiO₂ nanoparticles, T:G:A nanoparticles, XRD, FTIR, UV-Vis, FE-SEM

* Corresponding author: Vadamarathinam, yadamalarvnb@yahoo.co.in

1. Introduction:

Nanotechnology is emerging as a rapidly growing field with its application in both the nano-science and nano-technology in manufacturing new materials at the nano-scale range [1]. Titanium dioxide (TiO₂) is an inorganic white solid substance. TiO₂ oxide metal, is a chemically inert compound, which occurs in mineral sands and also in many kinds of Rocks naturally. In our tech-facilitated society Titania Nanoparticles have occupied an eminent place. Titanium IV Isopropoxide reacts with water to deposit titanium dioxide.



The processes involved in synthesizing Titania nanoparticles are important not only to find their applications in various fields but also to make them eco-friendly in nature[2-7]. In the due course of nanoparticle synthesis, attempts are being made to reduce the harmful reagents by amino acids[8]. Titanium dioxide has three forms of phases such as, Anatase, Brookite and Rutile. Anatase TiO₂ has wider industrial applications, exerts noticeable biological activity, more toxic than other Brookite and Rutile form of Titanium dioxide[9]. Glycine is the smallest non-essential, neutral and metabolically inert amino acid, with a carbon atom bound to two hydrogen atoms, and to an amino and a carboxyl group[10]. This amino acid is an essential substrate for the synthesis of several biologically important biomolecules and compounds[11]. It has a broad spectrum of anti-inflammatory, cytoprotective and immune-modulatory properties [12]. Alanine is α -amino acid that is used in the biosynthesis of proteins. It contains an amine group and a carboxylic acid group, both attached to the central carbon atom which also carries a methyl group side chain[13]. Glycine is a non-essential amino acid with various functions and effects which can bind to specific receptors and transporters that are expressed in many types of cells throughout an organism to exert its effects[14]. Attempt is made for the Titanium dioxide nanoparticle to penetrate bacterial cell membranes to reduce the toxicity[15].

2. Experimental Procedures

2.1. Preparation of Titanium Dioxide TiO₂ AND T:G:A Nanopowders:

Titanium (IV) Isopropoxide, Amino-acids (Glycine and Alanine), Ethanol, Ammonia (NH₃) Solution, De-ionized water, Acetone are used as precursors. All the chemical reagents used in our experiment were of analytical grade and were used as received without further purification. Firstly, Titanium (IV) Isopropoxide [0.5M] ratio is dissolved in 100 ml distilled water, kept in vigorous stirring for 45 minutes along with heat at 100°C continuously. The Titanium (IV) Isopropoxide reacts with H₂O to form the product of Titanium dioxide (TiO₂) pale white precipitate solution. This Homogeneous solution P_H range is noted as 7. Then, 2 drops of Ammonia is added to maintain the P_H range at 12. Now, the colloidal white precipitate solution is kept in undisturbed form with no stirring and heating process in order the Titanium dioxide TiO₂ precipitate settles down, leaving the water content on the top. The water content is sucked-out using the sucker. The settled TiO₂ precipitate is again washed with Distilled water, twice. For further purification, the product is washed with Ethanol solution, thrice. The Microwave irradiation was passed through TiO₂ white precipitate at 110° C for 35 minutes in Convectional Mode. Finally, obtained Pure Titanium dioxide TiO₂ Nano powder is annealed in muffled furnace at 400° C for 3hours. In the process of preparing T:G:A nanoparticle (precursors such as Glycine and Alanine), same process of preparing

pure titanium dioxide nanopowder is followed. The purified final nano-product T:G:A white precipitate was kept in microwave irradiation for 35 minutes at 110° C in Convectional mode. Finally, obtained Titanium dioxide influenced with Amino-acids (T:G:A) Nano powder is annealed in muffled furnace at 400° C for 3 hours.

The synthesized TiO₂ and T:G:A nano particles at high temperature (400°C) have been characterized by XRD, FTIR, UV, FESEM and Anti-bacterial analysis.

3. Results and Discussion

3.1. Structural Investigation of TiO₂ and T:G:A Nanoparticles By X-Ray Diffraction Analysis:

The crystalline phase of Titanium dioxide (TiO₂) and Titania influenced by Amino-acids (T:G:A) were confirmed from the peaks obtained in the X-ray diffraction pattern as shown in Figure 1.

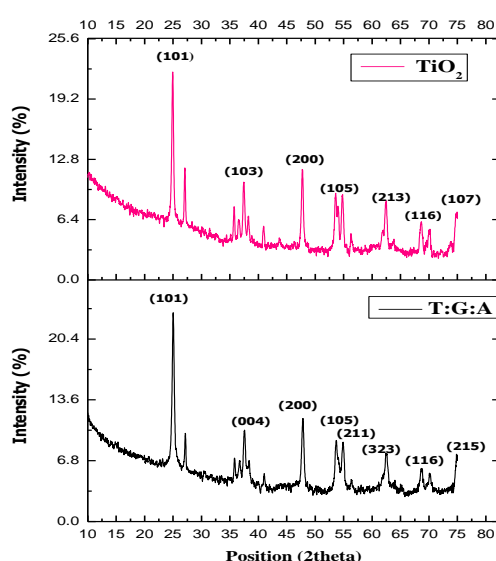


Figure 1. XRD Spectrum of TiO₂ and T:G:A Nanoparticles

3.11. Single Crystal X-Ray Diffraction:

The lattice parameters of synthesized TiO₂ nanoparticle is $a = b = 3.775 \text{ \AA}$, $c = 9.4902 \text{ \AA}$ and for T:G:A nanoparticle $a = b = 3.73 \text{ \AA}$, $c = 9.3700 \text{ \AA}$ ($a = b \neq c$). The lattice Angles for both TiO₂ and T:G:A nanoparticles agrees with $\alpha = \beta = \gamma = 90^\circ$ which indicates that both the synthesized nanomaterial has a Tetragonal Crystal structure. Due to the influence of Amino-acids, Intensity of XRD peaks have been increased shown in Figure 1.

3.12. Powder X-Ray Diffraction:

The broadened XRD peaks indicate that size of synthesized titania nanomaterials are very small which will be used in various industrial applications [16]. The experimental XRD pattern in Figure 1 shows an anatase phase of TiO₂ nanoparticles, it matches the orientation of the miller indices (hkl) to each peak for with JCPDS card number (#001-0562), these planes (101, 103, 200, 105, 213, 116, 107) are at the position of ($2\theta = 25.362^\circ, 37.973^\circ, 48.465^\circ, 53.892^\circ, 62.979^\circ, 69.212^\circ, 75.434^\circ$), (101) direction

represent the strongly peak (i.e., FWHM (β) for 100% peak) is determined at 24.9992° position. For T:G:A (anatase Phase) which is a meta-stable state [17], matches the orientation of the miller indices (hkl) to each peak for with JCPDS card number (#002-638), these planes (101, 004, 200, 105, 211, 323, 215) are at the position of ($2\theta = 25.552^\circ, 37.962^\circ, 48.225^\circ, 53.894^\circ, 55.299^\circ, 69.110^\circ, 75.434^\circ$), (101) direction represent the strongly peak (i.e., FWHM (β) for 100% peak) is determined at 24.9382° nanoparticles.

3.13. Crystallite Size (D):

From this study, the intensity of XRD peaks are positioned at degrees (2θ), average particle size of synthesized nanoparticles has been estimated using Debye-Scherrer formula. Inter-planar spacing between atoms (d-spacing) is calculated using Bragg's Law and the particle size are calculated from the expressions (1) and (2) enumerated in Table 1 and Table 2.

$$2d \sin\theta = n\lambda \quad (1)$$

$$D = 0.9\lambda / \beta \cos\theta \quad (2)$$

Where, D is the crystallite diameter size, λ is wavelength of X-Ray (0.15406nm), β is FWHM (Full-width half maximum intensity of the Peak), θ is diffracted angle incident X-ray on the sample. The Intensity of the TiO_2 increases after influencing amino acids in T:G:A nanoparticles with respect to Position (2θ) in degrees from Figure 1. By using Debye-Scherrer formula it is found that the average particle size has been decreased (from 32.97nm for TiO_2) due to the influence of Amino acids (28.90 nm for T:G:A). This is in agreement with DongxuZhou et al [18] reports that the reduction of Particle size results in increasing the stability of Nanoparticles.

3.14. Williamson-Hall Plot:

Williamson-Hall plot was used to estimate the crystallite size and lattice strain samples using the following formalism. The total broadening of the diffraction peak is due to sample and the instrument. The total broadening β_t equation is described by [18] expression (3),

$$B_t = B_{\text{Strain}} + B_{\text{Size}} = \left\{ \frac{K\lambda}{L \cos\theta} \right\} + \{4C\epsilon \tan \theta\} \quad (3)$$

Where ($C\epsilon$) is the lattice strain, L is average crystallite size, (B_{Strain}) is the strain broadening, B_{Size} is the particle size broadening, λ is the (1.5406 Å) X-ray wavelength, K is the dimensionless factor (0.9) and θ is Bragg angle in degrees. The equation (3) is multiplies by the $\cos\theta$ to yield,

$$B_t \cos\theta = 4C\epsilon \sin\theta + \frac{K\lambda}{L \cos\theta} \quad (4)$$

W-H plot is shown in Figure 2 and Figure 3. It is plotted by the graph of (B_t) $\cos\theta$ against $4\sin\theta$. The lattice strain ($C\epsilon$) of the sample from the slope (gradient). While the crystallite size can be estimates from intercept ($\frac{K\lambda}{L}$). Lattice Strain value is increased from 0.133 (TiO_2) to 0.60215 (T:G:A). This may be due to the quantum confinement effect. The strain value increases for decreasing the Crystallite size of both synthesized TiO_2 and T:G:A nanoparticles.

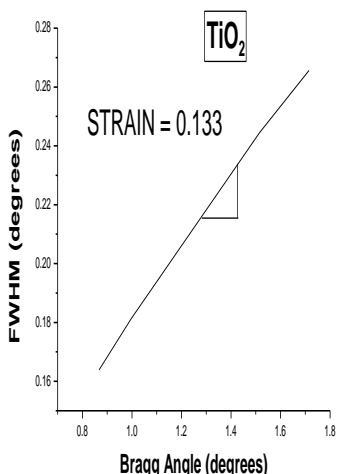


Figure 2. Williamson Hall plot for TiO₂

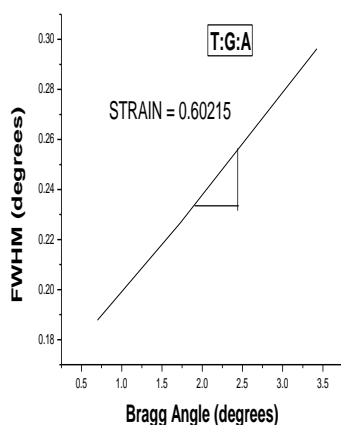


Figure 3. Williamson Hall plot for T:G:A nanoparticles

3.15. Specific Surface Area (SSA):

The Specific Surface Area (SSA) plays an important role in the nanoparticles due to their larger surface to volume ratio with a decrease in particle size. SSA is used to determine the type and property of nanoparticle [19]. SSA is used in various studies such as absorption, heterogeneous catalysts and reactions on surfaces. The average Specific Surface Area of Synthesized TiO₂ and T:G:A nanoparticles has been calculated by using equation (5) which is enumerated in the Table 1 and Table 2.

$$SSA = \frac{6000}{D \cdot \rho} \tag{5}$$

Where D is the Particle Size of the synthesized sample, ρ is the Density of NPs. Average Specific Surface Area is found to be 28.31 m²g⁻¹ for TiO₂ and 36.40 m²g⁻¹ for T:G:A as shown in Table 1 and Table 2. It is obvious that the specific surface area (SSA) increases when particle size (D) decreases, which reduces the pore size in the material[20]. In this study, the SSA of T:G:A nanoparticles is smaller than TiO₂ nanoparticles, which implies that the stability and hardness of the material increases for

T:G:A. Hence we can say the hardness and stability of TiO₂ increases [19] due to influence of amino-acids.

3.16. Dislocation Density (δ):

The Dislocation Density (δ) is the length of dislocation lines per unit volume of the crystal. Larger dislocation density implies a larger hardness [21] as shown in Table 1 and Table 2.

$$\delta = 1 / D^2 \tag{6}$$

Where, δ is Dislocation density, D is crystallite size of the samples, The Average Dislocation density (δ) of the synthesized sample using the expression (6) is determined as (1.51 X 10⁻³m⁻²) for TiO₂ and (1.06 X 10⁻³m⁻²) for T:G:A nanoparticles. From Figure 4(a) and Figure 4(b) it is clear that the dislocation density increases, when crystallite size is decreased which again confirms that the hardness and the strength of T:G:A nanoparticles is increases than pureTiO₂ nanoparticles.

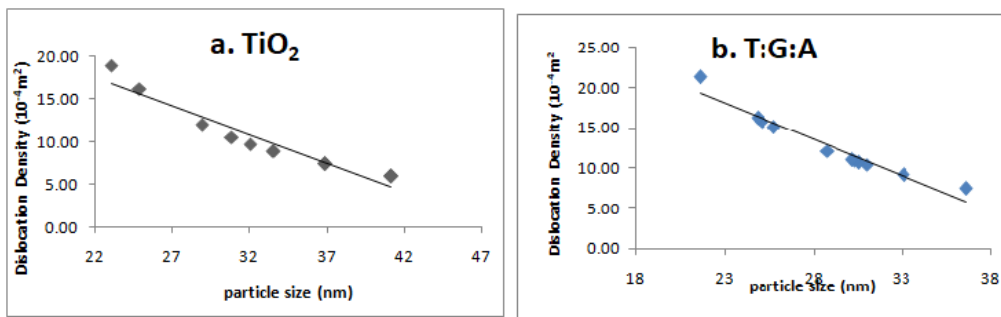


Fig.4.Dislocation Density Vs particle size of (a) TiO₂, (b)T:G:A

3.17. Morphology Index (M.I):

TiO₂ nanopowder is widely used in many diverse industries. Such applications are derived from its unique structural, physical and chemical properties, which are reflected by its hardness, surface properties, particle size and morphology. It is proposed that the specific surface area (SSA) of TiO₂ nanopowder depends on the interrelationships of particle morphology and size [22]. Morphological Index is obtained by using equation (7) the values obtained are enumerated in Table1 and Table 2, for both synthesized TiO₂ and T:G:A nanoparticles.

$$M.I = \frac{FWHM_h}{(FWHM_h + FWHM_p)} \tag{7}$$

Where, M.I is Morpholog Index, FWHM_h is highest FWHM value (Full width half-maximum intensity) from the peaks and FWHM_p is the particular peak’s FWHM for which M.I is to be calculated.

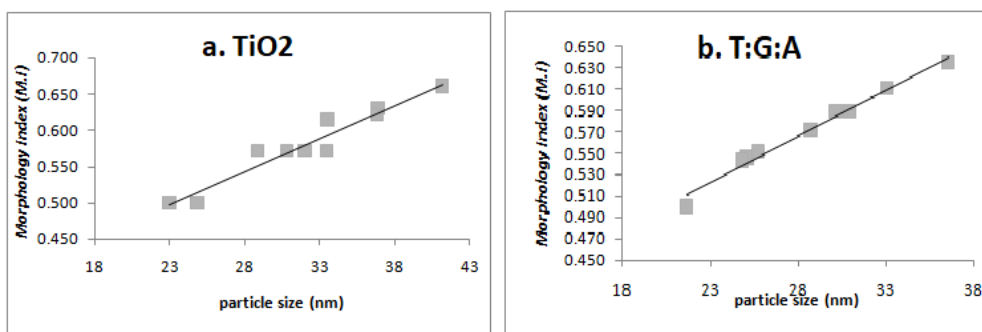


Fig.5.M.I vs. Size of Synthesized (a) TiO₂, (b) T:G:A

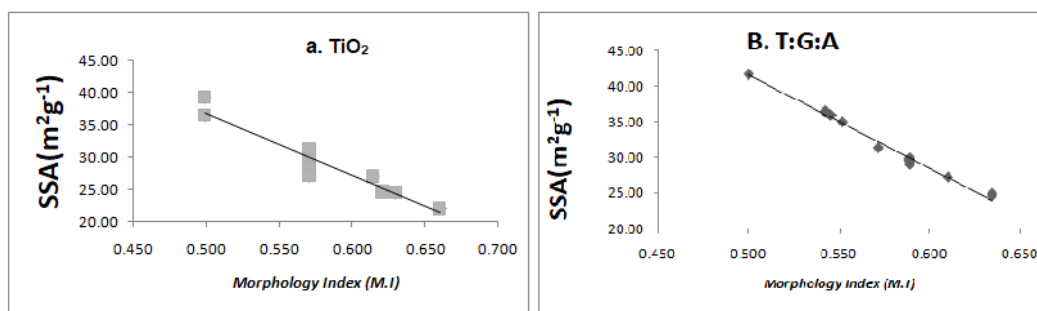


Fig.6.MI Vs SSA of Synthesized (a) TiO₂, (b) T:G:A

Figure 5 represents the graph between Morphological Index (M.I) and Crystallite size of the synthesized TiO₂ and T:G:A nanoparticles . Figure 6 indicates the graph between M.I and SSA of both synthesized TiO₂ and T:G:A nanoparticles. MI values falls in the range for TiO₂ nanoparticles is from 0.614 - 0.571 and for T:G:A nanoparticles is from 0.634– 0.543 which are obtained from expression using equation (7) presented in the Table1 and Table 2. It is observed that MI is directly proportional to particle size and inversely proportional to specific surface area with small deviations. The variation of MI vs Particle size Vs SSA are shown in Fig.5and Fig.6, where linear fit in the figure indicates the deviations and relationships between the three parameters (MI, SSA and Particle size). The observed results of the MI confirm the uniformity and fineness of the prepared nanoparticles.

3.18. Microstrain(ϵ):

Microstrain is the degree of distortion of lattice planes gives rise to non uniform changes in the interplanar spacings present in the crystalline lattice.

$$\epsilon = \frac{\beta}{4 \tan \theta} \quad (8)$$

where, β is FWHM (Full-width half maximum intensity of the Peak), θ is diffracted angle incident X-ray on the sample The application of defective TiO₂ nanoparticles are used in several applications than pristine TiO₂ nanoparticles [23]. Also the properties of TiO₂ can be fine-tuned precisely by tuning variations in their crystal structure like dislocation density, micro strains[24,25]. Usually annealing at high temperatures may stimulate the changes in their crystalline structure and microstrain due to change in their micro strain and hence change in stress. It is obvious that from Table 1 and Table 2, the influence of aminoacids plays a vital role in the micro strain values which may leads to affect its magnetic and opotical properties of T:G:A nanoparticles. These changes can also influence the light absorption properties of T:G:A which may induce photocatalytic applications.

Table 1: Particle size (D), Specific Surface Area (SSA), Morphology Index (M.I), Dislocation Density (δ) and Microstrain (ϵ) of TiO₂ Nanoparticles

Position [°2 θ]	FWHM β [rad]	D nm	SSA (m ² g ⁻¹)	MI (No Unit)	ϵ (10 ⁻⁴ m ²)	E (10 ⁻³)
24.9992	0.004237	33.52538	26.97	0.614	8.90	4.76
27.9759	0.003472	41.16201	21.96	0.660	5.90	3.47
35.9895	0.003472	41.16201	21.96	0.660	5.90	3.47
36.8768	0.003964	36.88404	24.51	0.630	7.35	2.96
37.7623	0.005072	28.90333	31.28	0.571	11.97	3.70
47.8952	0.00412	36.84658	24.54	0.621	7.37	2.31
53.9873	0.006764	23.02071	39.27	0.499	18.87	3.31
54.8912	0.005072	30.82778	29.33	0.571	10.52	2.43
62.6218	0.005072	32.0289	28.23	0.571	9.75	2.08
68.7543	0.006764	24.86512	36.36	0.499	16.17	2.46
70.2746	0.005072	33.47068	27.01	0.571	8.93	1.80
Average		32.9721	28.31	0.588	10.15	2.98

Table 2: Particle size (D), Specific Surface Area (SSA), Morphology Index (M.I), Dislocation Density (δ) and Microstrain (ϵ) of T:G:A Nanoparticles

Position [°2 θ]	FWHM β [rad]	D nm	SSA (m ² g ⁻¹)	MI (No Unit)	Δ (10 ⁻⁴ m ²)	E (10 ⁻³)
24.9382	0.003887	36.53999	24.74	0.634	7.49	4.38
27.0973	0.004314	33.06747	27.34	0.610	9.15	4.46
35.7891	0.005065	28.77716	31.42	0.571	12.08	3.91
36.8769	0.006745	21.6768	41.71	0.500	21.28	5.04
36.8769	0.004715	31.01053	29.15	0.589	10.40	3.53
31.6784	0.004715	30.57727	29.57	0.589	10.70	4.14
28.3478	0.004715	30.33864	29.80	0.589	10.86	4.65
25.8712	0.004715	30.18011	29.96	0.589	10.98	5.12
22.3945	0.005625	25.13276	35.97	0.545	15.83	7.08
22.3478	0.005485	25.77223	35.08	0.552	15.06	6.92
21.4754	0.005682	24.83849	36.40	0.543	16.21	7.47
Average		28.90	36.4	0.574	12.73	5.16

3.2. Fourier Transformation Infra-Red (FTIR) Analysis

The various intensities of vibrations indicating different types of compound classes and assessments obtained through number of ranges in the FTIR spectrum is shown below in Table 2. In the Fig. 7, FTIR spectra confirm the bond between O-Ti-O at around (605.65cm^{-1}) by the presence of Alkynes ($\equiv\text{C-H}$ bend) at Strong peaks of functional groups. FTIR spectrum for the Synthesized TiO_2 and T:G:A Nanoparticles is shown in the figure 7 and figure 8.

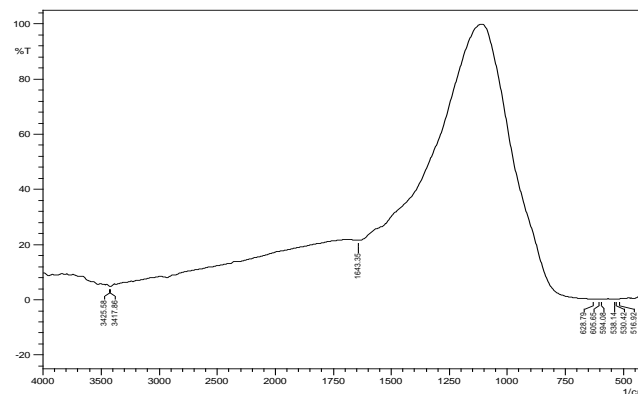


Figure 7. FTIR Spectrum for Synthesized TiO_2

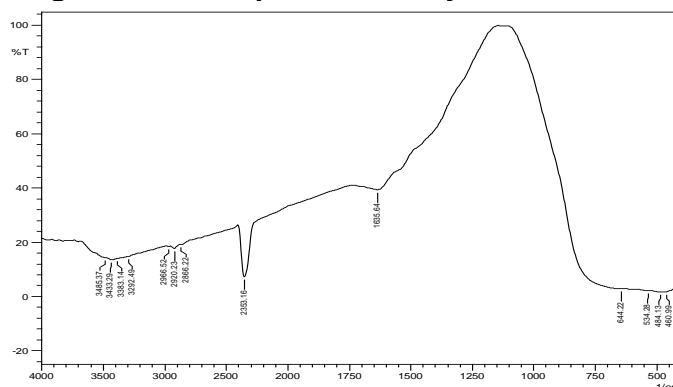


Figure 8. FTIR Spectrum for Synthesized T:G:A

From Figure 8, it is observed that the FTIR spectrum of synthesized T:G:A nanoparticles has various additional vibrations indicating the presence of amino-acids (Glycine and Alanine) as compared with synthesized TiO_2 Figure 7. The presence of Glycine in Strong(broad) intensities is confirmed at the range [2866.22cm^{-1}] by compound class Carboxylic acids (RCO_2H) structure and also in range [3383.14cm^{-1}] assigned in O-H, N-H stretch, H-bond by ($\text{C}=\text{CCOOH}$) structure. The presence of Alanine compound has been obtained in Strong, Medium and Narrow peak intensities at the range [3292.49cm^{-1}] assigned in [$=\text{C-H}$, $-\text{C}\equiv\text{C-H}$ stretches] by the class of Alkynes (terminal) and also in range [1635.64cm^{-1}] by class (1° Amines) at N-H bend (RCONHR) structure [26]. The Presence of TiO_2 is confirmed by the Strong peaks of functional groups at the range [534.28cm^{-1}] in the class of Alkyl halides (C-Br Stretch) [27], at [3433.29cm^{-1}] by Alcohols, Phenols and Ethers (OH stretches) [28] and at [2920cm^{-1}] Dimer OH by carboxylic acids (RCH_2CH_3) structure. The various functional groups at different

ranges and different compound class present at various intensities for the synthesized TiO_2 and T:G:A nanoparticles are found in this spectrum.

3.3. Ultra Violet-Visible (UV-Vis) Analysis:

The optical properties of TiO_2 depend strongly on the type of material (e.g., single crystal, powder) and the synthesis conditions[29]. From the Figure 9, the cut-off wavelength starts early from 222nm for TiO_2 and increases to 232nm for T:G:A nanoparticle. It shows the UV-Visible absorption spectra of Titanium dioxide (TiO_2) and T:G:A nanoparticles recorded in the wavelength region 200–800 nm. The energetic band structure and the energy band gap of the prepared TiO_2 and T:G:A nano particles have been determined using optical absorption spectra. The absorption coefficient (α) is related to the band gap (E_g) by the following expression,

$$(\alpha h\nu)^2 = B (h\nu - E_g)^n \quad (9)$$

$$E_g = \frac{h*c}{\lambda} \quad (10)$$

$$I = I_0 e^{-\alpha t} \quad (11)$$

Where, (h) is the plank's constant (6.626×10^{-34} Js), (α) is the absorption coefficient, (c) is the speed of light ($3.0 \times 10^8 \text{ms}^{-1}$), (λ) is Cut-off wavelength (410.57×10^{-9} m), (ν) is the photo frequency, (B) is a constant, (I) is the intensity of transmitted light, (I_0) is the intensity of incident light and (t) is the thickness of the sample.

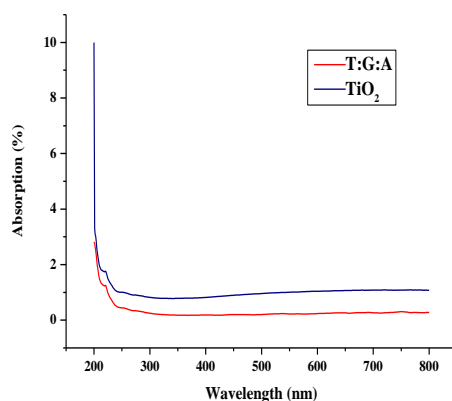


Figure 9. Optical Absorption Spectrum of TiO_2 and T:G:A

Figure10 and Figure 11 represents the Tauc plots of Direct and Indirect Energy Band Gap for both TiO_2 and T:G:A nanoparticles, comparatively. From figure10 direct band gap energy E_g for TiO_2 is 5.6eV is shifted to 4.9 eV after influenced with Amino-acids (T:G:A). Similarly indirect band gap energy for TiO_2 is also shifted from 5 eV to 4.5 eV due to the impact of addition of amino-acids (T:G:A) as shown in figure 11. When the particle size reaches the Nano scale, every particle is made-up of very small number of atoms and molecules. When the number of over-lapping of orbitals (or energy-level) decreases and the width of band gap E_g gets narrower. This reduction in its bandgap may be due to the decomposition of amino acids results in excitation of surface plasmons. Due to the quantum confinement effect, band gap of the nanoparticles decreases when the particle size decreases which leads to the electrons confinement resulting the reduction of

band gap at the chemical level [30]. Hence T:G:A nanoparticles may give more possibilities in design and optimisation of photonic and optoelectronic devices.

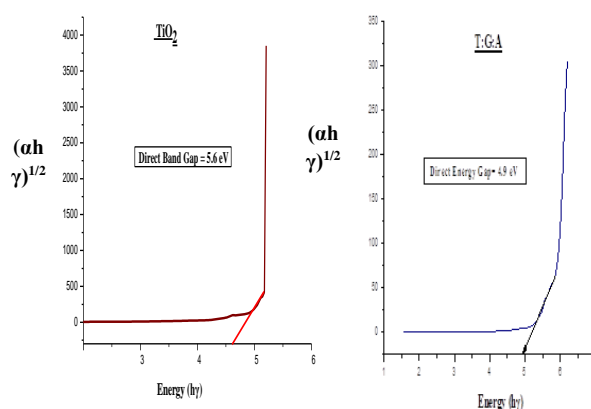


Figure 10. Tauc Plots of Direct Energy Band Gap (a) TiO₂, (b) T:G:A

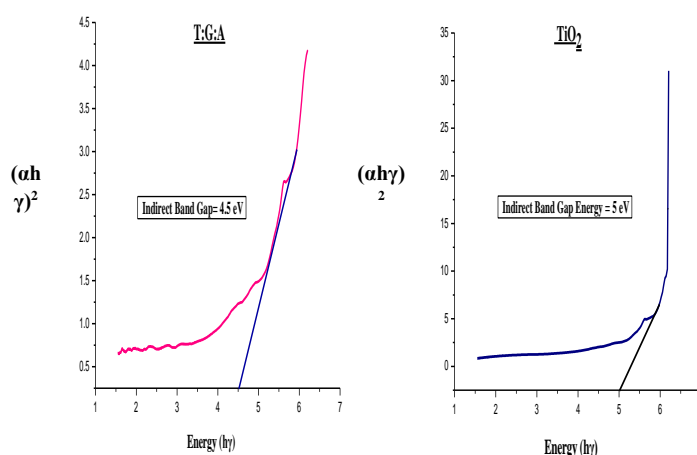


Figure 11. Tauc Plots of In-Direct Energy Band Gap (a) TiO₂, (b) T:G:A

3.4. Field Emission Scanning Electron Microscope (FESEM) Analysis:

The morphological survey of synthesized TiO₂ and T:G:A Nanoparticles were studied using the FESEM and a typical picture is presented in the figure 12 and figure 13. The nanoparticles were in agglomerated state and found to be in spherical shape also found in the cluster format. Erdemong et al [31] also reports that the size of TiO₂ Nanoparticles around (30-36nm) have circular in shape. The morphology of synthesized TiO₂ and T:G:A Nanoparticles are shown with high magnification under the analysis of FESEM. The high magnified image carried out under different micrometrical range 1 μ m, 2 μ m and 200 nm, respectively. It is observed that T:G:A nanoparticles more denser than TiO₂ Nanoparticles which are assembled on the surface in 200nm magnification.

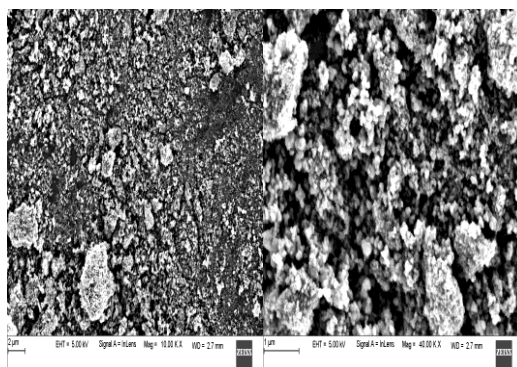


Fig.12-FE-SEM Micrographs of TiO₂ (a) 2μm, (b) 1μm.

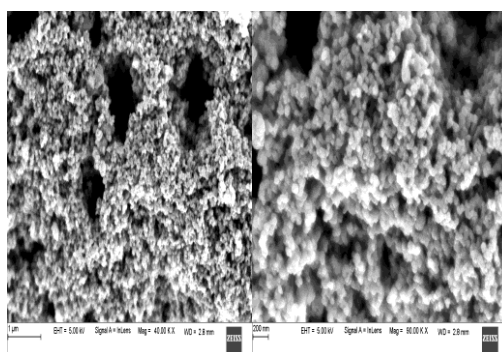


Fig.13-FE-SEM Micrographs of T:G:A (a) 1μm, (b) 200nm.

4. Conclusion:

The structural investigation and characterization of pure TiO₂ and T:G:A nanoparticles are studied. The hardness and the strength of TiO₂ nanoparticles have been enhanced due to the impact of Amino-acids (T:G:A) which is confirmed by X-Ray Diffraction studies. From the UV-Vis study, it is conformed that renormalisation of band gap due to the decomposition of aminoacids into plasmons leads to the various applications in optoelectronic, photoconductive and photocatalytic properties. FESEM studies confirms that the changes in density of T:G:A. Hence, the High Efficiency and Eco-friendly Titanium dioxide influenced with Glycine and Alanine (T:G:A) nanoparticles have been synthesized as cost effective with short span of time as compared to other synthesising techniques.

References:

- [1] Dr. Pallab Ghosh, Associate Professor, Department of Chemical Engineering, IIT Guwahati, "Introduction to Nanomaterials & Nanotechnology, Interfacial Engineering Module 9: Lecture 1-NPTEL"
- [2] Alagarasi.A, Indian Institute of Technology Madras | IIT Madras · NCCR, Department of Chemistry, "Introduction to Nanomaterials, Chapter: 1", (2011) pp.76
- [3] A.M.H. Milad , L.J. Minggu, M.B. Kassim, M.Yoshihara, "Progress in Photoelectrochemical water splitting research", Ceramic International. Vol 39, (2013), pp 3731-3739.

- [4] K.Shanthi, P.Manikandan, C. Rani, S.Karuppusamy, “Synthesis of nanocrystalline titanium dioxide for photodegradation treatment of remazol brown dye” *Appl.Nanoscience*. vol 5, (2015), pp 373-378.
- [5] N. Suzuki, S.Karuppusamy, S. Ito., “Uniform coating of a crystalline TiO₂ film onto steel plates by electrochemical deposition using staged pulse current”, *J. Appl. Electrochem.*, Vol 39, (2009), pp 141-146.
- [6] Chou-Yi Hsu, Zaid H. Mahmoud, Sherzod Abdullaev, Farah K. Ali, Youssef Ali Naeem, Rabaa Mzahim Mizher, Manal Morad Karim, Alzahraa S. Abdulwahid, Zahed Ahmadi, Sajjad Habibzadeh, Ehsan Kianfar, “Nano titanium oxide (nano-TiO₂): A review of synthesis methods, properties, and applications”, *Case Studies in Chemical and Environmental Engineering*, vol 9, (2024), pp. 100626.
- [7] KulandaisamyAJ¹, Rayappan JBB¹, “Significance of Nanoparticles and the Role of Amino Acids in Structuring Them-A Review”, *J NanosciNanotechnol.*, vol 18(8), (2018), pp 5222-5233.
- [8] R M Hobson 1, B Saunders, G Ball, R C Harris, C Sale, “Effects of β-alanine supplementation on exercise performance: a meta-analysis”, *Amino Acids*. Vol 43(1), (2012), pp 25-37.
- [9] Yazhi. A.S.,Guarda, G,Riteau, N. Drexeler, S.K., Tarivel, A., Couilin. I and T.Scopp. J., “Proceedings of the National Academy of sciences of the united states of America”, vol 107(45) (2010).
- [10] M.A. Henderson, “A surface science perspective onTiO₂ photocatalysis”, *Surf.Sci. Rep.* 66, 185 (2011).
- [11] P. Bowen, H. Hofmann, M. Staiger, R. Steiger, P-A.Brugger, and K. Peternell, “Colloidal processing of nanoceramic powders for porous ceramic film applications”,DOI:10.4028/Key Eng.Mater206-213.1977Corpus ID: 135612601
- [12] Jason P. Tierney, PelleLidström, “Microwave Assisted Organic Synthesis”, (2005).
- [13] Alagarasi.A, Indian Institute of Technology Madras | IIT Madras · NCCR, Department of Chemistry, “Introduction to Nanomaterials, Chapter: 1”, (2011), pp. 21-26.
- [14] Aguayo-Cerón KA, Sánchez-Muñoz F, Gutierrez-Rojas RA, Acevedo-Villavicencio LN, Flores-Zarate AV, Huang F, Giacomani-Martinez A, Villafañá S, Romero-Nava R., “Glycine: The Smallest Anti-Inflammatory Micronutrient”, *Int J Mol Sci.*, vol 24(14) (2023), pp. 11236. doi: 10.3390/ijms241411236.PMID: 37510995 **Free PMC article.**
- [15] Unfried. K, Albercht .C, Klotz.L.O, Von Milkecz.A, Grether-Beck. S, and Schins, R.P.F., “Cellular Responses to Nanoparticles: Target Structures and Mechanism Nanotechnology”, vol 1 (2007), pp52-71.
- [16] K. Vijayalakshmi* and D. Sivaraj, “Synergistic Antibacterial activity of barium doped TiO₂nanoclusters synthesized by microwave processing”, *RSC Adv.*, vol 6, (2016), pp. 9663–9671.

[17] J Hanaor DAH, “Sorrel CC (2011) Review of the Anatase to rutile phase transformation”, *J Mater sci* 46:855-874.

[18]. Dongxuzhou, Zhaoxiaji, Xingmaojiango Dorren R. Donphy, Jeffrey Brinker and Arturo A. Keller, “Influence of material properties on TiO₂ nanoparticles agglomeration, Articles from public library of science”, *Plos One*, vol 8(11), (2013), e81239.

[19]. Omer Kaygili, NiyazBulut, CengizTalar, TankutAter, Turanince, “Sol-Gel Synthesis And Characterization of TiO₂ Powder”, *International journal of Innovation Engineering Application*, vol 1(2), (2017), pp. 38-40.

[20] ThirugnanasambandanTheivasanthi* and MarimuthuAlagar, “Titanium dioxide (TiO₂) Nanoparticles XRD Analyses: An Insight”, *Chemical Physics*, (2013) <https://doi.org/10.48550/arXiv.1307.1091>

[21] Monuko du Plessis, “Relationship between specific surface area and pore dimension of high porosity nanoporous silicon – Model and experiment”, *physica status solidi (a) – applications and materials science (pss a)*, vol 204(7), (2007), pp. 2319-2328.

[22] E.Kumar, D.Muthu Raj, S.C.Velladuroi, S.Karthiga Devi, A.JenufaBegam, “Synthesis and Structural Investigations of Titanium Dioxide (TiO₂) Nanoparticles By Microwave Assisted Method”, *International Research Journal of Engineering and Technology (IRJET)*, Vol 2(9), (2015), pp. 458-461.

[23] Yanqin Li, Wei Wang, Fu Wang, Lanbo Di, Shengchao Yang, Shengjie Zhu, Yongbin Yao, Cunhua Ma, Bin Dai and Feng Yu, “Enhanced Photocatalytic degradation of Organic Dyes via defect-rich TiO₂ prepared by dielectric Barrier discharge plasma”, *Nanomaterials*, vol 9(5), (2019), pp. 720.

[24] K.M. Prabu, S. Perumal, “Micro Strain and Morphological studies of Anatase and Rutile Phase TiO₂ Nanocrystals prepared via sol-gel and solvothermal method-comparative study”, *International journal of Scientific Research in Science, Engineering and Technology*, vol 1(4), (2015), pp. 299-304.

[25] O. Wiranwetchayan, S. Promnopat, T. Thongtem, A., “Chaipanich – effect of polymeric precursors on the properties of TiO₂ films prepared by sol-gel method”, *Mater.Chem. Phys.*, vol 240 (9), (2020), pp. 122219, <https://doi.org/10.1016/j.matchemphys.2019.122219>

[26] Ghosh SC, Thanachayanont C, Dutta J., “Studies on Zinc sulphide nanoparticles for Field Emission Devices. The 1st ECTI Annual Conference (ECTI-CON 2004)”, Pattaya, Thailand, (2004), May 13-14; p.145-148.

[27] Mamoru Senna, Nicholas Myers, Anne Aimable, Vincent Laporte, Cesar Pulgarin, Oualid Baghriche and Paul Bowen, “Modification of titania nanoparticles for photocatalytic antibacterial activity via a colloidal route with glycine and subsequent annealing”, *J. Mater. Res.*, Vol 28(3), (2013), pp. 354–361.

[28] Archana Kapoor and Anu Malik, "Beta-alanine: Design, synthesis and antimicrobial evaluation of synthesized derivatives", *Der Pharmacia Lettre*, vol 8 (12), (2016), pp. 135-142.

[29] Ibrahim. A, Abdul-Hassan, Ahmed K.Abbas, IsamM.Ibrahim and ZinahS.Shallal, "Characterization and Antimicrobial Effects of Titanium dioxide Nanoparticles Produced by Laser Ablation", *Vol 8(49)*, (2018), pp. 14286-14292

[30] Yu-Hui Chen, Ronnie R. Tamming, Kai Chen, Zhepeng Zhang, Fengjiang Liu, Yanfeng Zhang, Justin M. Hodgkiss, Richard J. Blaikie, Boyang Ding & Min Qiu, "Bandgap control in two-dimensional semiconductors via coherent doping of plasmonic hot electrons", *Nature Communications*, vol 12, (2021), Article number: 4332

[31] Erdemog˘lu, N., Ku˘ Peli, E., Yes, E., Ilada, R. 2003. Anti-inflammatory and antinociceptive activity assessment of plants used as remedy in Turkish folk medicine. *J. Ethnopharmacol.*, vol 89(1),(2003), pp. 123-1, doi: 10.1016/s0378-8741(03)00282-4